Chinese Chemical Letters 33 (2022) 4505–4516

Contents lists available at ScienceDirect

Chinese Chemical Letters

journal homepage: www.elsevier.com/locate/cclet

Fluorescence resonance energy transfer-based nanomaterials for the sensing in biological systems

Xiaotong Shen[a,b], Wei Xu[a,*], Jin Ouyang[b], Na Na[b,*]

[a] School of Life Science, Beijing Institute of Technology, Beijing 100081, China
[b] Key Laboratory of Radiopharmaceuticals, Ministry of Education, College of Chemistry, Beijing Normal University, Beijing 100875, China

ARTICLE INFO

Article history:
Received 24 August 2021
Revised 10 October 2021
Accepted 22 December 2021
Available online 27 December 2021

Keywords:
Nanomaterials
Fluorescence resonance energy transfer
Nano-sensors
Detection
Biochemical processes

ABSTRACT

The applications of fluorescence resonance energy transfer (FRET) are coming to be one of the simplest and most accessible strategy with super-resolved optical measurements. Meanwhile, nanomaterials have become ideal for constructing FRET-based system, due to their unique advantages of tunable emission, broad absorption, and long fluorescence (FL) lifetime. The limitations of traditional FRET-based detections, such as the intrinsic FL, auto-FL, as well as the short FL lifetime, could be overcome with nanomaterials. Consequently, numbers of FRET-based nanomaterials have been constructed for precise, sensitive and selective detections in biological systems. They could act as both energy donors and/or acceptors in the optical energy transfer process for biological detections. Some other nanomaterials would not participate in the energy transfer process, but act as the excellent matrix for modifications. The review will be roughly classified into nanomaterial-involved and uninvolved ones. Different detection targets, such as nucleic acids, pathogenic microorganisms, proteins, heavy metal ions, and other applications will be reviewed. Finally, the other biological applications, including environmental evaluation and mechanism studies would also be summarized.

1. Introduction

The applications of fluorescence resonance energy transfer (FRET) in biological detections have been dramatically increased in recent years. FRET is coming to be one of the simplest and most accessible strategy with super-resolved optical measurements [1–8]. The FRET-based detections have provided multiple information based on changes of intra- and intermolecular distance in the scale of nanometers [9–14]. Normally, the FRET system consists of pairs of matched fluorophores, which are defined as donor and acceptor fluorophores, respectively. The premise of FRET requires the emission of the donor fluorophore overlaps the excitation of the acceptor one. Thereafter, when two fluorescent chromophore groups are close enough, the donor absorbs photons of a certain frequency, and is excited to a higher electron energy state. Subsequently, before the electrons return to the ground state, the energy is transferred to the neighboring acceptor through the interaction of dipole. Simultaneously, FRET occurs, whose transferred energy would subsequently result in the quenching of the original donor fluorophore or another excitation for the acceptor emission. FRET will occur when more than 30% donor emission overlaps with the absorption of the acceptor, whose distance is less than 10 nm [15].

Based on these changes of the emission, the biological detections would be obtained combined with special interactions with biological targets. Consequently, applications of FRET in the life sciences have increased dramatically over the past twenty years [16–19]. In general, FRET has been applicable for variety applications at the molecular levels. For example, it can be used for monitoring of environment changes (temperature, ionic strength, *etc.*) [20] and examining the interactions between molecules (aggregation or cleavage) [21,22]. However, for FRET-based sensing in biological systems, design and selection of fluorescence (FL) groups still encounter limitations and shortcomings for further applications in life science.

Firstly, when excited by light photons, mitochondria and lysosomes can release energy in the form of photons, which leads to auto-FL [23]. Moreover, intrinsic cell FL, auto-FL and the emission from the undesired compounds can also interfere with FRET signals, which would definitely lead to deviations. Thus, mixed signals including emissions from biological systems were normally

* Corresponding authors.
E-mail addresses: weixu@bit.edu.cn (W. Xu), nana@bnu.edu.cn (N. Na).

https://doi.org/10.1016/j.cclet.2021.12.061
1001-8417/

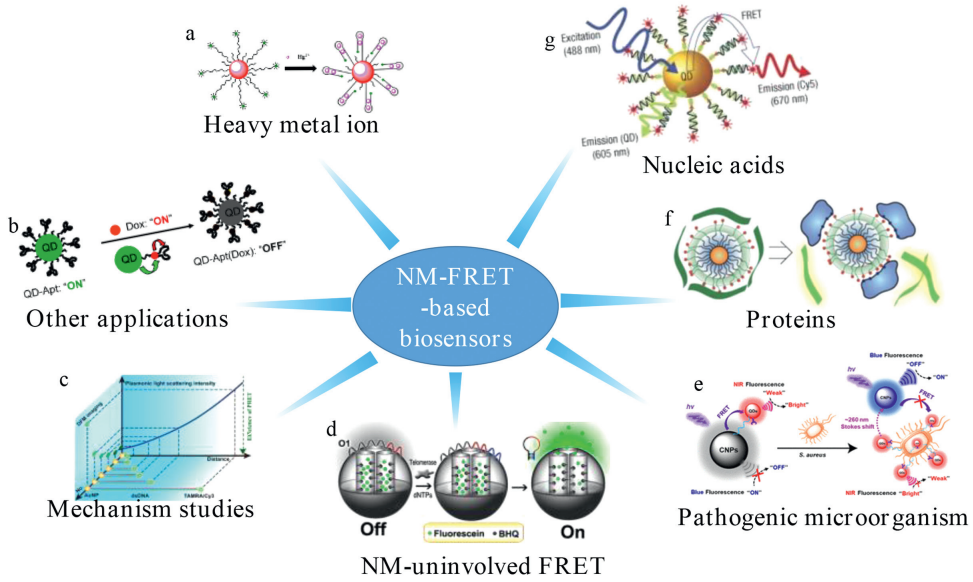

Scheme 1. FRET-based nanomaterials for the sensing in biological systems. (a) Reproduced with permission [32]. Copyright 2015 Elsevier B.V. (b) Reproduced with permission [116]. Copyright 2007, American Chemical Society. (c) Reproduced with permission [120]. Copyright 2020, American Chemical Society. (d) Reproduced with permission [46]. Copyright 2013, American Chemical Society. (e) Reproduced with permission [96]. Copyright 2020, American Chemical Society. (f) Reproduced with permission [33]. Copyright 2007, Macmillan Publishers Ltd. (g) Reproduced with permission [30]. Copyright 2005, Nature Publishing Group.

recorded, which could lead to errors in biological monitoring. Secondly, traditional FRET-based molecules normally have a short FL lifetime. Once these FRET-based molecules are excited, they can only keep excited for a very short period of time. Under the brevity measurement of the emission, auto-FL would take up a significant percentage of the recorded emissions. This would overlap the interesting emissions to affect reliable biological examinations [24,25]. Therefore, the traditional FRET-based techniques need the further improvement to match the precise biological detections.

With the development of material science, materials at the nanoscale have become one of the most prominent techniques. Especially, nanomaterial-based biosensors have exhibited their unique advantages for precise, sensitive and selective detections in biological systems [26,27]. Nanomaterials are ideal for FRET due to their tunable emission, broad absorption, and long FL lifetime. They are more adaptable for applications than the event of single acceptor fluorophore with one excitation. Consequently, FRET-based nanomaterials with unique optical signals have become a new challenge to design sensors for biological detections. The introducing of nanotechnology techniques into constructing of FRET-based biosensors would overcome the shortcomings mentioned above. In addition, nanomaterial-based applications take advantage of the preferential accumulation of nanomaterials for detections in tumor tissues. Besides, combining with the improvement of fluorophores, new FRET-based nanomaterials have been developed for precise and sensitive biological detections in life science.

At present, the nanomaterials used for constructing FRET-based system normally include quantum dots (QDs) [28–31], gold nanoparticles (AuNPs) [32–35], graphene oxide (GO) [36–41], DNA nanostructures [42–44], mesoporous silicon nanoparticles (MSNs) [45–48], *etc.* These nanomaterials can act as both energy donors and/or acceptors in the optical energy transfer process. During this process, signal changes or quenching would be recorded for biological detections. In addition, some nanoparticles (such as MSNs) would not participate in the FRET, but act as the excellent matrix for the maintaining FRET process. They are still active for selective detections after special modifications. In comparison to traditional FRET system, the designing of nanomaterial-based FRET system is more challenged and variable for different targets, including nucleic acids, proteins, pathogenic microorganisms, heavy metal ions, *etc.* In addition, the FERT-based nanomaterials can also be applied into the dynamic examination or mechanism studies of FRET. The overall summary of applications is given in Scheme 1.

In this review, we will give an insight into the development of FRET-based nanomaterials for biological detections. Considering whether the nanomaterials are involved in FRET process, the review will be roughly classified into nanomaterial -involved and uninvolved ones. We will mainly introduce nanomaterial-involved FRET process for different detection targets, such as nucleic acids, pathogenic microorganisms, proteins, heavy metal ions and other detections. Finally, the other biological applications, including environmental evaluation and mechanism studies would also be summarized.

2. Nanomaterials involved FRET processes

In recent years, nanomaterials involved in FRET have been particularly widely used, especially when they were functionalized as both donors and acceptors [49–52]. Based on unique optical properties and their potentials as carriers, FRET-based nanomaterials have gained wide attentions for biosensing in biological systems. The main applications on the nanomaterial-involved FRET detections will be reviewed for different target detections.

2.1. Detection of nucleic acids (in vitro & in vivo)

2.1.1. In vitro applications

The detection of nucleic acids is of central importance for biological applications, including clinical diagnosis, detection of infectious agents and biowarfare agents. For the simple and sensitive detection of nucleic acids, induced fluorescence resonance energy transfer (iFRET) was particularly suitable based on DNA hybridization. In iFRET, the acceptor is covalently linked to an oligonucleotide probe to form a double-stranded DNA (dsDNA). The donor, such as Sybr Green I, can emit fluoresces during interacting with dsDNA. Hybridization of the probe with its complement induces excitement of the donor dye and the subsequent energy transfer to the acceptor dye. The energy transfer process concomitant to

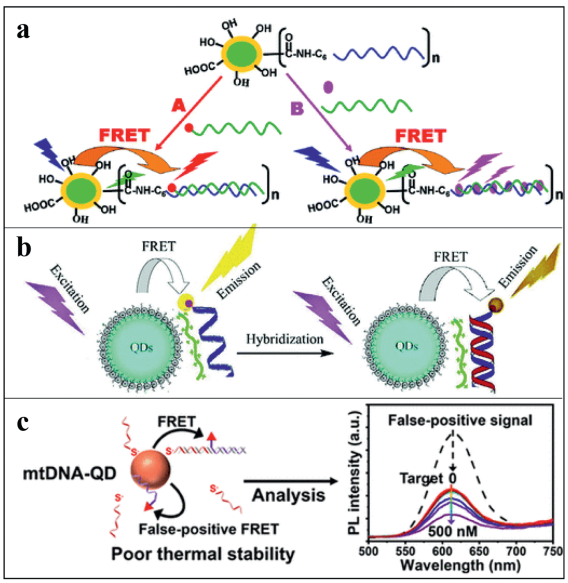

Fig. 1. (a) A compact functional QD-DNA conjugate: Preparation, hybridization, and specific label-free DNA detection. Copied with permission [57]. Copyright 2008, American Chemical Society. (b) DNA hybridization detection with blue luminescent QDs and dye-labeled ssDNA. Copied with permission [59]. Copyright 2007, American Chemical Society. (c) Subnanomolar FRET-based DNA assay using thermally stable phosphorothioated DNA-functionalized QDs. Reproduced with permission [61]. Copyright 2019, American Chemical Society.

hybridization status can therefore be easily monitored *via* the FL output of the acceptor dye. Considering the reversible interaction with the donor dye is employed *via* dsDNA, this iFRET technique is extremely useful in nucleic acid detection [53].

An earlier iFRET-based nanomaterial for the detection of DNA was designed by Zhang *et al.* [54]. In this iFRET system, streptavidin-modified CdSe/ZnS QDs with photoluminescence emission at 605 nm acted as the donor and Cy5 fluorophore acted as the acceptor. Based on the sandwich hybrid, Cy5-labeled reporter was complementarily bound to biotinylated capture with the presence of targeted DNA. Thus, *via* strong streptavidin biotin affinity, this hybrid was driven toward QDs surface to form the iFRET system. As established, 54 hybrids could be self-assembled on an individual QD, significantly increasing the FRET efficiency to achieve 4.8 fmol/L of limit of detection (LOD). This was much sensitive compared to the molecular beacon (MB) method with LOD of 0.48 pmol/L. Furthermore, combined with an oligonucleotide ligation assay, a biosensor was designed for detection of a point mutation in ovarian tumors [55]. Later, for improving detection sensitivity of QD-FRET-based DNA sensor, Zhang *et al.* have conducted the QD-based single-molecule detection system in a capillary flow. The system exhibited significant improvements, which related to FRET efficiency, photobleaching prevention, higher sensitivity and lower sample consumption (5 orders of magnitude less). Compared to FRET in bulk solution, greater FRET efficiency was obtained due to the deformation of DNA in the capillary stream [56].

For the detection of DNAs by FRET-based sensors, the specificity and sensitivity are still limited by nonspecific DNA adsorption and poor colloidal stability during hybridization. To overcome these limitations, Zhou *et al.* have designed 11-mercaptoundecyl tri(ethylene glycol) alcohol (EG_3OH)/11-mercaptoundecyl tri(ethylene glycol) acetic acid (EG_3COOH)-capped QDs (Fig. 1a). The EG_3 group provided surface stabilization as well as prevention of non-specific DNA adsorption. Target DNA was covalently attached to the (EG_3OH)/(EG_3COOH)-capped QDs through carboxyl-to-amine crosslinker and was used as energy donor. A594 labeled complementary DNA acted as energy acceptor in the designed system. Moreover, the DNA-attached (EG_3OH)/(EG_3COOH)-capped QDs could also be used for the detection of non-labeled complementary DNA aided by a dsDNA intercalating dye (such as Ethidium bromide (EB). For example, during the hybridization, EB was intercalated into the double-strand hybrid to fabricate FRET system between QD and EB. Therefore, with this system, both labeled and non-labeled DNA can be successfully detected with sensitivity of 1 nmol/L on a conventional fluorimeter [57].

Furthermore, the multiple detection and recognition of DNAs have also been employed by the FRET-based system. For example, with two different QDs as donors and EB as energy acceptor, Algar *et al.* have designed FRET system for multiple detection of DNAs. Briefly, QD-FRET-based sensors consisted of green/red mercaptoacetic acid (MAA) capped CdSe/ZnS QDs and Cy3/A647 labeled DNA, for simultaneous detection of two different target DNA [58]. More simply, based on the electrostatic attraction, the proximity between the donor and the acceptor can also be achieved to enable FRET. Based on this idea, a cationic polymer of poly (diallyldimethylammonium chloride) acted as an electrostatic linker between blue thioglycolic acid (TGA)-capped CdTe QDs and Cy3-labeled ssDNA (Fig. 1b). The two QDs acted as energy donor and acceptor, respectively. With the target DNA, FL of QD/Cy3-ssDNA decreased, due to the more rigid structure of dsDNA (a hybrid of target DNA and ssDNA) to increase the energy transfer distance. Subsequently, different hybridization of DNAs with different FRET efficiencies was well recognized, for their different interactions with the polymer [59].

In addition, decreased photoluminescence was normally observed due to QDs aggregation by hybridization, normally achieved through ligand modifications. For example, Lee *et al.* have prepared a positively charged dihydrolipoic acid (DHLA)-2,2-(ethylenedioxy)bis(ethylamine) derived ligand and polyethylene glycol-modified CdSe/ZnS QDs. Therefore, an electrostatic complex between the QDs and negatively charged TAMRA-ssDNA was fabricated. Upon this strategy, QDs aggregation was avoided due to charge neutralization after hybridization [60]. More recently, phosphorothioated single-stranded DNA (pt-ssDNA) acted as a multivalent ligand for DNA-functionalization, which stabilized DNA/QD interface for FRET-based DNA assay (Fig. 1c). With this strong multivalent binding of pt-ssDNA to the surface of QDs, the detachment of pt-ssDNA and nonspecific adsorption of DNA were successfully prevented. This detection was specifical and sensitive, showing LOD of 0.47 nmol/L, about 30 times lower than conventional monothiolated ssDNA-capped QDs (16.1 nmol/L) [61].

Theoretically, the structural conformation of DNAs has great impact on DNA-nanoparticle conjugates to fabricate FRET system. Therefore, the orientation, function, and length of DNA on nanoparticle surfaces at low nanomolar concentrations should be examined under physiological conditions. Consequently, Guo *et al.* investigated the conformations of a 31 nt DNA attached to a semiconductor QD. Different FRET conformations were obtained during hybridization of Tb-DNA probes to different positions of DNA on the QDs. The precise Tb-to-QD distances from 7 nm to 14 nm were determined by time-resolved FRET spectroscopy, which was obtained from a 26 nt peptide-appended QD-DNA. Eleven different distances/configurations of the same QD-DNA conjugates were examined. The denser conformation of ssDNA was therefore confirmed, which possibly possessed more flexible orientation on the QD surface. Whereas, the dsDNA was fully extended with radial orientation [62]. To further investigate DNA-DNA interactions and ligation in FRET, a DNA origami nanostructure was selected as a model to specifically mimic a DNA double-strand break (DSB) (Fig. 2). The end-joining of two fluorescently labeled DNAs, with the T4 DNA ligase on the single-molecule level, were studied based on

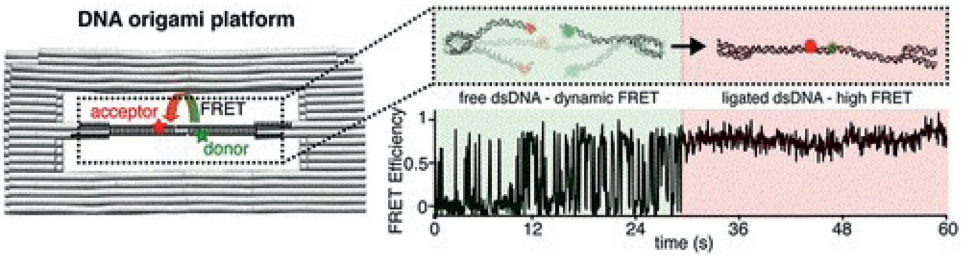

Fig. 2. A DNA Origami platform for single-pair FRET investigation of DNA−DNA interactions and ligation. Copied with permission [63]. Copyright 2020, American Chemical Society.

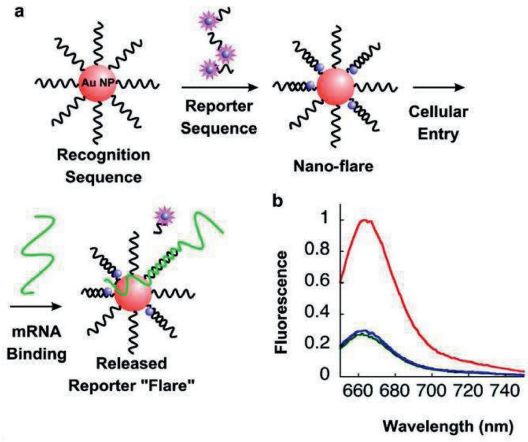

Fig. 3. (a) Nanoparticles functionalized with a recognition sequence are hybridized with a short complementary Cy5 labeled reporter strand, which is capable of being displaced by the target. (b) FL spectra of 1 nmol/L nano-flares alone (green), in the presence of 1 μmol/L target (red), and in the presence of 1 μmol/L noncomplementary sequence (blue). Reproduced with permission [64]. Copyright 2007, American Chemical Society.

monitoring of ligation reactions. Before ligation, dynamic fluctuations of FRET signals were observed under transient binding of sticky overhangs. Then, the FRET signal became static after the ligation. Therefore, the ligation reactions were monitored *via* transition from dynamic to static FRET process in solution and on surface-anchored origamis [63].

2.1.2. In vivo applications

Applying FRET-based technique to *in vivo* applications has obtained great attentions for their potentials in diagnosis. To achieve diagnosis based on FRET-based FL imaging, the *in vitro* behavior of nanomaterials was normally examined. While the *in vitro* FRET-based assays could not always be effective for cancer development and metastasis. Therefore, appropriate nanoprobes required to be constructed and examined for FRET-based sensing in cells or even *in vivo*. Some advances on detection of intracellular nucleic acids are present as follows.

In 2007, a spherical nucleic acid (SNA) AuNP-based platform (the NanoFlare) was fabricated for the FL detection of the mRNA transcript of the oncogene survivin. As shown in Fig. 3, AuNPs were functionalized with thiolated. The oligonucleotides with an 18-base recognition element achieved a specific RNA transcript *via* the formation of gold thiol bond. Then, oligonucleotide-functionalized AuNPs hybridized with short Cy5-labeled reporter sequences, showing flares when displaced by a longer target. At the bound state, the Cy5 signals from the reporter strand were quenched when they were closed to the AuNPs surface. In the presence of a target, the flare strand was displaced and liberated from the AuNPs. This process formed the longer and more stable duplex between the target and the oligonucleotide-modified AuNPs [64]. With the highly oriented, dense oligonucleotide coating, NanoFlares entered cells efficiently without using cytotoxic transfection agents [65–69]. Unlike FISH probes, this method did not require fixation of cells prior to analysis [70]. In addition, treating cells with NanoFlares, no obvious cytotoxicity [71,72] was observed, which enabled detections of small genetic molecular contents in living cells [73].

To detect trace amounts of target molecules *in vivo*, the nucleic acid amplification technique was introduced into FRET-based detection. For example, by single-stranded tile (SST) self-assembly, a self-assembled, spatially addressable SST nanostructure was constructed as a DNA nano-manipulation platform. Based on DNA strand displacement technology, the fluorescent dye was pre-assembled in the nano-manipulation platform. Then, the energy was transferred to the destination. The photonic logic circuits were achieved by FRET signal cascades, including logic AND, OR, and NOT gates. Thus, this transfer process was successfully validated by visual DSD software [74].

Currently, the FRET-based imaging of intracellular mRNA normally confronted intrinsic interferences, which generated from complex biological matrices to result in inevitable errors. Thus, some DNA nanostructures have been constructed to circumvent this problem during intracellular imaging. For example, Tan *et al.* developed a DNA tetrahedron nanotweezer (DTNT) to image tumor-related mRNA in living cells based on the FRET off to on signals. As shown in Fig. 4a, with target mRNA, the distance between two fluorophores on adjacent DTNT tips decreased to emit FL signals under FRET. With this DTNT, the cancer cells were intracellularly distinguished from normal cells based on mRNA expressions. This FRET-based nanoprobe almost entirely avoided intrinsic interferences, such as nuclease digestion, protein binding and thermodynamic fluctuations in complex biological matrices [42].

Subsequently, series DNA nanostructure-based FRET system have been evoked for wider applications. Combined with DNA assisted cyclic amplification, Gao *et al.* constructed a DNA tetrahedron nanoprobe (DTNP)-based FRET sensing platform (termed DTNP sensor) for sensitive detection of tumor-related miRNA. With this platform, the expression levels and the inhibition of hsa-miR-146b-5p expression in different cell lines were evaluated successfully [43]. Simultaneously, a split G4 nanodevice assembled by DNA frameworks was fabricated to realize FRET-based microRNA imaging in living cells [44]. Furthermore, the intracellular dual detections have also been achieved using DTN-based FRET probe. Zhu *et al.* proposed a DNA tetrahedral-based FRET probe for monitoring both pH and tumor-related mRNA in living cells (Fig. 4b). This was employed by designing fluorescent reporters, which combined advantages of pH-responsive DNA triplex structure and signal amplification strategy (HCR). In the presence of target survivin mRNA, the HCR was triggered between free H1 and H2 to generate long dsDNA. This drew the FL donors and acceptors close to each other and resulted in a FRET-based manifesting signal for sur-

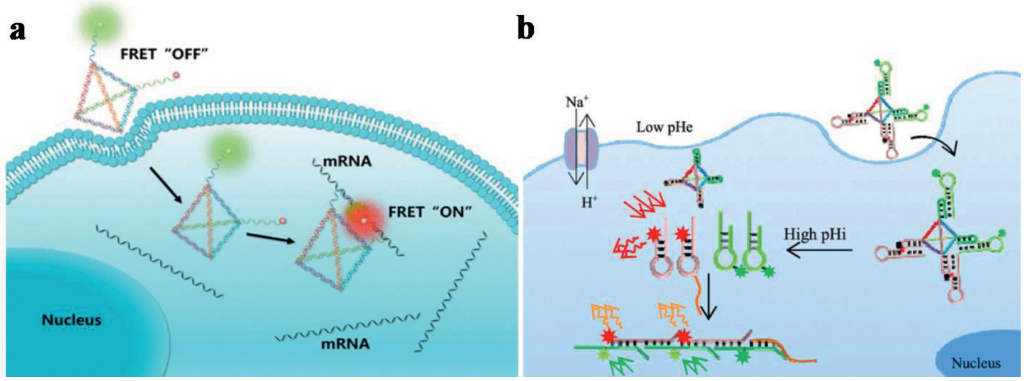

Fig. 4. (a) FRET-based DNA tetrahedron nanotweezer for highly reliable detection of tumor-related mRNA in living cells. Copied with permission [42]. Copyright 2017, American Chemical Society. (b) DNA tetrahedral-based FRET nanoprobe for imaging of intracellular pH and tumor-related mRNA. Copied with permission [75]. Copyright 2019, American Chemical Society.

vivin mRNA detection. The LOD of survivin mRNA was 0.035 nmol/L [75].

2.2. Detection of proteins

The expression of certain biomarker proteins and/or irregular proteins can indicate the disease states. The sensitive, convenient and precise detection of proteins has provided crucial tools for early diagnosis and treatments. While the protein's structural diversity and complexity are main challenges for protein detections [33]. Currently, the most extensively used method for protein detection is the enzyme-linked immunosorbent assay (ELISA) [76]. Despite its high sensitivity, the high cost, instability and quantification still challenge the wide application of this method.

Currently, many probes have been designed to image intracellular biomarkers for diagnosis. However, most probes normally confront intrinsic interferences from complex biological matrices to result in inevitable false-positive signals. To circumvent this problem, AuNPs-based biosensors have been fabricated. AuNPs can act as FL quenchers for their strong absorbance. This would definitely endow sensors with lower background than those utilizing organic fluorophore quenchers. For example, a sensor array containing six noncovalent AuNPs-fluorescent polymer conjugates was constructed to detect proteins [33]. The AuNPs' end groups carried additional hydrophobic, aromatic or hydrogen-bonding functionalities to tune interactions between AuNPs and polymer/proteins. Simultaneously, AuNPs associated with charge-complementary fluorescent dyes to produce quenched complexes *via* FRET. Thus, the subsequent binding of proteins displaced the dyes and regenerated the FL. The sensitivity was highly improved due to the high surface area of the AuNPs. Then, distinct signal response patterns can be obtained by modulating the nanoparticle-protein and/or nanoparticle-dye association. This strategy was successfully used to differentiate 52 unknown proteins with an accuracy of 94.2%, which demonstrated the feasibility of nanomaterial-based arrays for protein differentiations.

Although FL-based sensing has been widely explored for biological detections, the overlapped emission still limited the further applications. To overcome the emission-overlapping caused by small Stokes shifts and wide emission spectra, Wang *et al.* designed a AuNPs-based dual-labeled FRET biosensor. This sensor was applied to simultaneously detect matrix metalloproteinases (MMPs) in living cells. For sensing, a cleavable peptide spacer was fabricated onto the surface of AuNPs through cysteine residues, which comprised of an MMP-2 substrate of Gly-Pro-Leu-Gly-Val-Arg-Gly [34] and an MMP-7 substrate of Val-Pro-Leu-Ser-Leu-Thr-Met-Gly [35]. A lanthanide complex of BCTOT-EuIII (BCTOT = 1,10-bis(5-chlorosulfo-thiophene-2-yl)-4,4,5,5,6,6,7,7-octafluorodecane-1,3,8,10-tetraone) was attached onto the N terminus of the peptide, and 7-amino-4-methylcoumarin (AMC) was attached onto the C terminus of the peptide (Figs. 5a and b). Thus, the FRET system between labeled dyes and AuNPs was constructed. During FRET, a well-quenched nanoprobe was constructed, which readily resumed emission in the presence of one or both of the MMPs. With the presence of MMP-2 and MMP-7, the FRET system was destructed, which recovered FL signals at 449 nm and 613 nm under single wavelength excitation. The strategy has high specificity for simultaneous imaging of dual components in a complex system, and can effectively avoid negative outcomes in cancer cell diagnosis [77].

In fact, for FRET-based detection of proteins, QDs have shown great potentials based on their unique structural and optical characterizations. In 2012, Algar *et al.* demonstrated that QDs can be functionalized in a simultaneous role as both acceptors and donors within time-gated FRET relays. For applications, QDs were co-assembled with a long lifetime luminescent terbium (III) complex (Tb) or a fluorescent dye (Alexa Fluor 647, A647) labeled peptides or oligonucleotides. As shown in Figs. 5c and d, within the FRET relay, the QD served as a critical intermediary platform for two processes. Firstly, an excited-state Tb donor transferred energy to the ground-state QD, which followed a suitable microsecond delay. Secondly, the QD subsequently transferred that energy to an A647 acceptor for the detections. This approach can eliminate background FL. Moreover, two approximately independent FRET mechanisms were carried out simultaneously. This system employed in a single QD-bioconjugate to achieve multiplexed-biosensing *via* temporal resolution without requiring multiple colors of QD [78].

Furthermore, immunoassay strategy was also introduced into QD-based FRET system for protein detections. Wei *et al.* developed an QD-FRET-based in-solution sandwich fluoroimmunoassay to detect estrogen receptor beta (ER-β antigen). ER-β is a tumor suppressor that is down-regulated in the later stages of various cancers and can be used to monitor treatment efficacy [79–81]. For the detection, ER-β antigen was incubated with QD-labeled anti-ER-β monoclonal antibody and AF labeled anti-ER-β polyclonal antibody, forming a sandwich FRET-based immunoassay. Similarly, Wegner *et al.* designed an immunoassay that utilized a terbium-QD-based FRET system to detect cancer biomarkers. In this case, six different primary antibodies were used to bind a model biomarker (PSA) [82], enabling PSA detection at concentrations as low as 1.6 ng/mL [79]. Kim *et al.* developed a QD-based sandwich immunoassay on a glass substrate of vertical zinc ox-

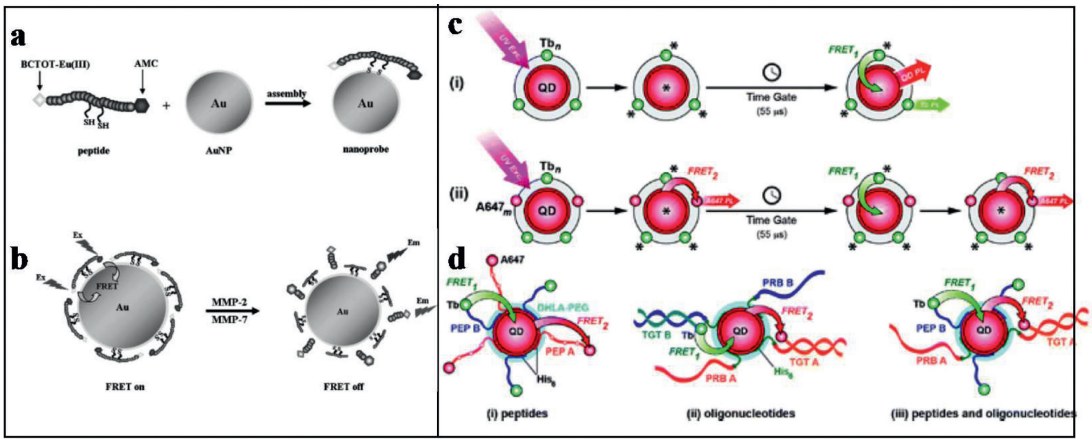

Fig. 5. (a, b) Construction of MMP-2 and MMP-7 assay with the nanoprobe and the sensing mechanism. Copied with permission [77]. Copyright 2012, Wiley. (c, d) QDs as simultaneous acceptors and donors in time-gated FRET relays. Copied with permission [78]. Copyright 2012, American Chemical Society.

ide (ZnO) nanowire array for carcinoembryonic antigen (CEA) detection [83]. The ZnO nanowire substrate provided a large surface area with many binding sites for binding of antibodies to the analyte of interest. With the presence of CEA, FRET occurred between ZnO nanowires and QD-labeled antibodies upon sandwich formation. Thereafter, the FL enhancement for detecting CEA was quantified using FL microscopy, which exhibited a large dynamic range (from 0.001 ng/mL to 100 ng/mL).

Furthermore, for the easy immunoassay-based detection, Ge *et al.* developed a paper-based immunosensor device. Combined with the fabrication of a QD-FRET system, AFP, CA 125, CA 15–3 (a biomarker derived from mucins that is used to detect tumor recurrence in breast cancer patients) [84–87], and CEA were successfully detected with detection limits of 0.3 pg/mL, 6.1×10^{-5} U/mL, 2.9×10^{-4} U/mL, and 1.4 pg/mL, respectively [88]. As shown in Fig. 6a, the immunosensor array was prepared by covalently immobilizing capture antibodies on corresponding working zone on a disposable paper array. Upon a sandwich-type immunoreaction, CuO NPs-labeled secondary antibody (Ab_2) bioconjugates were captured in each working zone. Next, dithizone (DZ)-quenched CdTe QDs were added on the sensor surface. Subsequently, the sensors were treated with HCl, which released Cu^{2+} from the CuO NPs. Finally, the FL of QD was recovery for the detection.

In fact, more and more species in complicated biological samples required to be detected. Recently, the multiple detection of proteins has attracted more attentions. In order to realize simultaneous detection and screening of multiple proteins, a 3D DNA nanostructure based on multistep QD-FRET has been exploited. As shown in Fig. 6b, the tetrahedron-structured DNA was constructed by four oligonucleotide strands and was subsequently conjugated to a streptavidin-coated QD. This realized the obtaining of a QD-Cy3-Texas Red-Cy5 tetrahedron DNA. This QD-Cy3-Texas Red-Cy5 tetrahedral DNA nanostructure has well-defined dye-to-dye spacing and high controllability for energy transfer between intermediary acceptors and terminal acceptors. Therefore, multistep FRET between the QD and three dyes (Cy3, Texas Red, and Cy5) was generated for simultaneous detection of multiple endonucleases and methyltransferases. In addition, the detection can also be employed for detecting complex biological samples as well as the screening of multiple enzyme inhibitors [41].

The FRET-based techniques can also be used for the special biological detections. For example, Yang *et al.* designed a nanoprobe based on QD-FRET to detect telomerase activity in cells. As shown in Fig. 6c, the QD-FRET-based nanoprobe consisted of a specific sequence of DNA, which were labeled with QD to act as a fluorescent donor. Simultaneously, A488 acted as a fluorescent acceptor, which resulted in the quenching of FRET-based FL signals under the complementarity to telomere repeats. Thus, with the presence of telomerase, the FRET system was destructed to make the FL signals on. Therefore, based on the recovery of FL signals, this DNA nanoprobe can achieve sensitive detection of telomerase even in single cell. In addition, the quantitative detection of telomerase activity in different numbers of cells was also achieved [89].

Moreover, the FRET-based system can also be used for tissue analysis and diagnosis. For instance, a FRET system of matrix metalloproteinase MMP 14-activated NIR-II nanoprobe (A&MMP@Ag_2S-AF7P) was constructed for rapid unperturbed-tissue analysis. Based on the FRET-based tissue analysis, the *ex vivo* and *in vivo* neuroblastoma diagnoses have been achieved. As shown in Fig. 6d, A&MMP@Ag_2S-AF7P displayed negligible FL in normal tissues due to the formation of FRET system. However, the emission of Ag_2S would be recovered upon inhibiting the FRET between Ag_2S-QDs and A1094. This process was mediated by MMP14 overexpressed in neuroblastoma. With this system, the lesion and tumor margins can be well-defined based on the instant illumination. Thus, the nanoprobes can be acted as a rapid diagnostic reagent for cancer surgical or tissue biopsy procedures [90].

2.3. Detection of pathogenic microorganisms

Pathogenic microorganisms are becoming increasingly serious worldwide problems, acting as causative agents of various infectious diseases. To treat pathogenic infection, the rapid and accurate detection of pathogenic microorganisms is of great importance [91]. The most popular methods to confirm the presence of pathogens microorganism are typically based on culture and colony counting methods. However, the culture and colony counting methods are less selective and more time intensive. Thus, there is an urgent need to construct biosensors that allowed easy-to-use, rapid, multiplexed, rapid and sensitive detection with a high signal-to-noise ratio for general pathogen detection.

For the sensitive detection of pathogenic microorganisms, amplification strategies are effective. For example, based on hybridization chain reaction (HCR), Tan *et al.* established a triplex DNA-based FRET system for rapid and specific detection of trace DNA sequences from vibrio parahaemolyticus (VP). As shown in Fig. 7a, the fluorescent arboxyfluorescein (FAM, donor) and tetramethylrhodamine (TAMRA, receptor) were labeled on triplex forming oligonucleotide (TFO) and hairpin sequence H1, respectively. In the present of VP DNA target, the hairpin structure of MB was opened. Then, the free end was released and hybridized with H1-TAMRA. This triggered the HCR reaction by the alternate supplementation

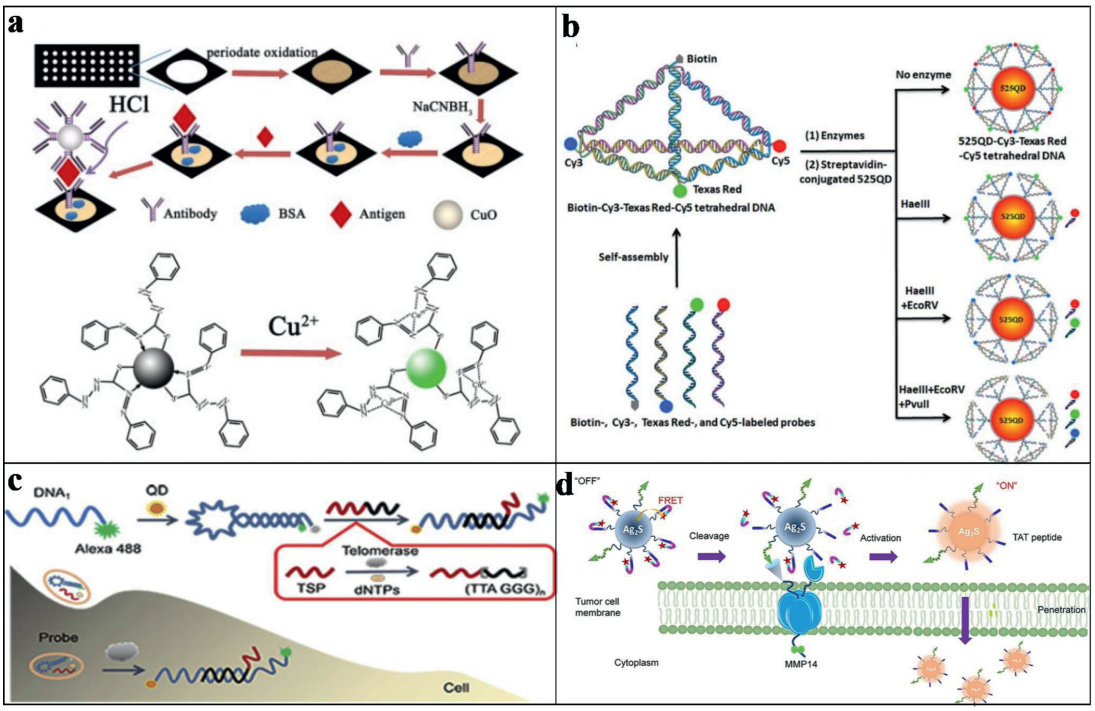

Fig. 6. (a) Schematic representation of preparation of "turn-on assay" of immunosensor. Copied with permission [88]. Copyright 2012, Elsevier. (b) Schematic illustration of the assembly of the 525QD-Cy3-Texas Red-Cy5 tetrahedron DNA nanostructure for multiple enzymes assay. Copied with permission [41]. Copyright 2019, American Chemical Society. (c) Schematic illustration of the DNA nanoprobe based on QD-FRET for telomerase sensing. Copied with permission [89]. Copyright 2019, Elsevier. (d) Schematic illustration of A&MMP@Ag_2S-AF7P for NB detection. Reproduced with permission. Copied with permission [90]. Copyright 2020, Wiley.

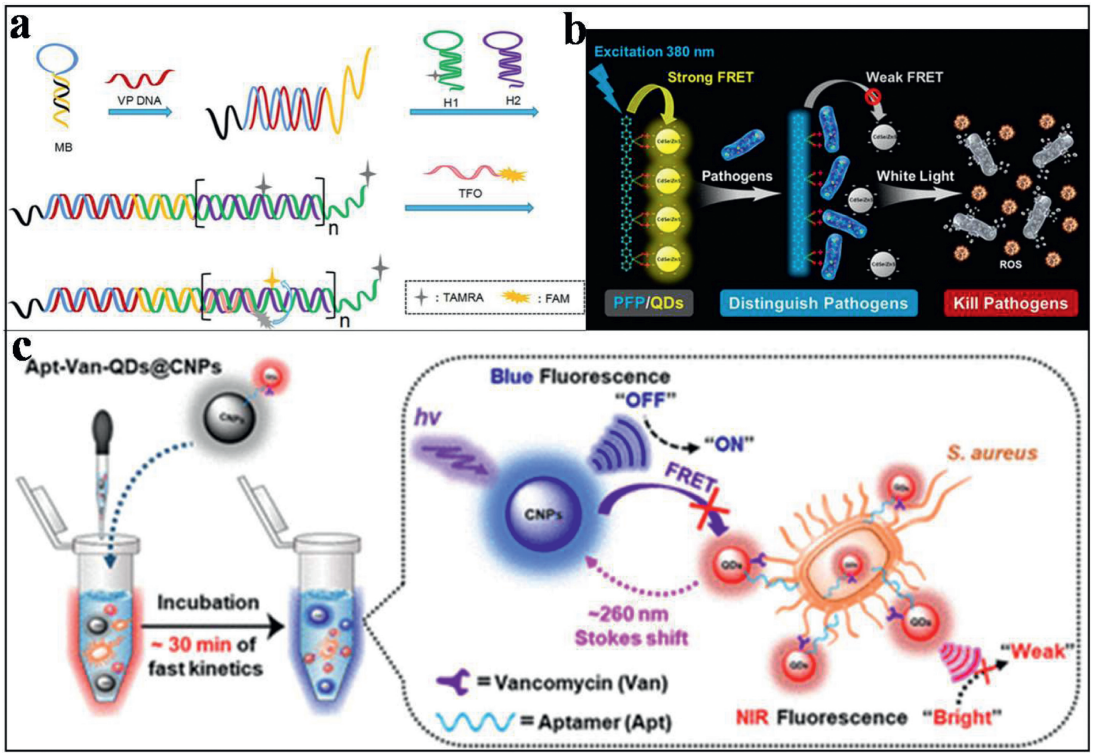

Fig. 7. (a) An enzyme free FRET strategy based on hybrid chain reaction and triplex DNA for Vibrio parahaemolyticus. Copied with permission [92]. Copyright 2020, Tan *et al.* (b) Schematic illustration of PFP/QD complex to achieve pathogen identification and antimicrobial capabilities. Copied with permission [95]. Copyright 2020, American Chemical Society. (c) Design of the vancomycin and aptamers (Apts) dual-recognition moieties-based ratiometric fluorescent nanoprobe. Copied with permission [96]. Copyright 2020, American Chemical Society.

of H1-TAMRA and H2 to produce the notch double helix analogue. With the addition of TFO-FAM, a triplex structure was formed between HCR products (H1-TAMRA/H2) and TFO-FAM. Therefore, the FRET system was constructed under the close contact between the donor and the receptor. *Via* the HCR amplifications, the FL quenching value was inversely proportional to the concentration of target VP DNA in the range of 0.1–50 nmol/L, and the LOD was 35 pmol/L [92].

Notably, with the development of QDs nanomaterials, polymer QD-based FRET system also showed advantages for the detection of pathogenic microorganism. As reported, polymer QDs exhibited excellent characteristics as fluorescent probes, including their extraordinary FL brightness, fast emission rate, excellent photostability, as well as nonblinking and nontoxic features [93,94]. Hence, Yuan *et al.* designed a new platform for pathogen discriminations and killings using FRET-based hybrid materials of conjugated polymer-QDs. As shown in Fig. 7b, the hybrid material was constructed through the electrostatic interaction between water-soluble anionic CdSe/ZnS QDs and a cationic poly(fluorene-alt-phenylene) (PFP) derivative. Thus, efficient FRET between PFP and QDs was promoted. Therefore, upon addition of different pathogen strains, the FRET from PFP to QDs was interrupted because of the competitive binding between PFP and the pathogens. In addition, complexation of PFP and QDs also reduced the dark toxicity to a more desirable level. Therefore, the controllable killing of pathogens was potentially realized [95].

With the development of nanomaterials, multifunctional roles, such as multiple recognition, multiple detections and even treatments have been implanted into FRET-based systems. For example, Shen *et al.* reported an integrated properties of a remarkably large Stokes shift and dual-recognition into a single matrix. This was applied to develop a ratiometric fluorescent nanoprobe for pathogenic microorganism stimuli-responsive detection. As demonstrated in Fig. 7c, the FRET occurred when the blue carbon nanoparticles (CNPs, energy donor) and NIR Apt-vancomycin (Van)-QDs (energy acceptor) became close. This led to a remarkable quenching of blue FL signal of CNPs at 465 nm and a NIR FL enhancement for Apt-Van-QDs at 725 nm. With this platform, the Apt-Van-QDs@CNPs system showed an ultrahigh specificity for ratiometric FL detection of *S. aureus*. A good LOD of 1 CFU/mL was therefore resulted, which allowed the assay at single-cell level. This work offered a new insight into the rational design of efficient ratiometric nanoprobes for rapid and on-site accurate screening of pathogenic microorganisms. This would be effectively employed at the single-cell level in the early stages, especially during the worldwide spread of COVID-19 today [96].

2.4. Detection of heavy metal ion

With the increasing of environmental pollution, mercury ion (Hg^{2+}) can pass through the food chain, and thereby accumulate in biological systems of human beings. As a toxic ion, Hg^{2+} tends to accumulate in central nervous system. Even trace amounts of Hg^{2+} would cause motor disorders, language and hearing impairment, limb deformity, swallow difficulty and even death in severe cases [97,98]. Therefore, the detection of Hg^{2+} in biological system has come to be an important issue to attract extensive interests. Currently, there are some traditional approaches for detecting Hg^{2+}, including mass spectrometry, atomic absorption spectroscopy, X-ray absorption spectroscopy, atomic FL spectroscopy, *etc.* Nevertheless, to obtain the real and *in situ* monitoring of Hg^{2+} in biological system, the simple, low cost, sensitive and biocompatible methods are required [99–103]. Recently, with the development of optical nanomaterials and FRET-based techniques, several efforts have been employed for detection of Hg^{2+} in biological systems.

One of the most widely used nanomaterials for FRET-based system construction is Graphene oxide (GO). GO has recently emerged as a fascinating material with special structural characterizations, such as one-atom thick, two-dimensional graphitic carbon structure [36,37] and various surface oxygen-containing groups including carboxyl, hydroxyl and epoxy groups [38]. These properties make GO be attractive for various biological applications [39,40]. Especially, for constructing FRET-based GO system, GO could act as a quencher to result in changes of FL intensity for detecting Hg^{2+}. For example, with GO as the absorption matrix, the signal changes of fluorescent carbon QDs absorbed on GO surface have been applied for Hg^{2+} detection. Briefly, Yang *et al.* modified multi-Ts in DNA sequences by fluorescent QDs, which would form FRET system to lead to FL quenching once DNA sequences absorbed on GO surface (Fig. 8a). With Hg^{2+} added, the conformation of DNA changed based on the interaction of T-Hg^{2+}-T, which broke the FRET system to recovery the FL signals. Therefore, the sensitive detection of Hg^{2+} was achieved with a LOD of 2.6 nmol/L, which was selective over a wide range of other metal ions [104]. Similarly, GO also gave a special contribution on adsorbing dye-labeled oligonucleotides *via* hydrophobic and π-π stacking interactions [105]. This simultaneously quenched the FL signals of dyes based on FRET. With the presence of Hg^{2+}, the competitive interaction between Hg^{2+} and oligonucleotides also released dye-labeled oligonucleotides from GO. Therefore, the FL signals recovered to result the sensitive detection of Hg^{2+} with low background.

The GO based FRET detection of Hg^{2+} was further evaluated by comparing the physical adsorptions and the covalent modification on GO surface. For the covalent modification, the amino-terminus of multi-T single-chains with FL were covalently linked to the carboxyl group on the GO surface *via* 1-ethyl-3-[3-dimethylaminopropyl] carbodiimide hydrochloride (EDC) coupling. Then, the two GO-FRET systems were applied to detect Hg^{2+}. When Hg^{2+} combined with mult-T DNA, the $[Hg(T)_2(H_2O)_2]_n$ could quench the FL (550 nm) of GO, indirectly revealing Hg^{2+} concentrations [106]. Furthermore, the covalent modified pathway was more stable and sensitive than the simple physical adsorbed method. The limits of detection were 20.6 nmol/L and 16.3 nmol/L, respectively [107].

Furthermore, Hg^{2+} can also be indirectly detected based on changes of FL intensity from other nanomaterials. For example, Li *et al.* immobilized single-stranded multi-T sequence on the surface of graphite carbonitride (g-C_3N_4). Then, based on the construction of FRET system, the FL of gC_3N_4 was quenched with the presence of Hg^{2+}, which realized the detection of Hg^{2+} [108]. Moreover, Chen *et al.* used WS_2 to adsorb the single-stranded multi-Ts sequence. The quenching of FL would be observed based on the construction of FRET system. Thus, with the FRET-based sensors, Hg^{2+} can be detected in nmol/L level [109].

Moreover, some other nanomaterials, such as AgNPs, Ag nanoclusters (AgNCs) or AuNPs, can also act as FL donor or quencher to construct FRET system for detecting Hg^{2+}. For example, a FRET system was prepared by growing of AgNP on FAM-labeled DNA strand. This resulted greatly quenched FAM signals under the protection of AgNPs by DNA [110]. As shown in Fig. 8b, With the addition of Hg^{2+}, Ag/Hg amalgam was formed to suppress the AgNPs growth on the DNA. This led to the interrupt of FRET system, which made the FL signal of FAM recovered. Therefore, the enhancement of FL intensities can be used for the detection of Hg^{2+} at the a few nanomolar level.

Similarly, AuNPs can also be applied into constructing FRET-based system for Hg^{2+} detection. As shown in Fig. 8c, single-stranded DNA labeled with FAM was immobilized on the AuNPs [32]. With this configuration, the FRET system was constructed with quenched FAM signals when FAM closed to the surface of AuNP. Subsequently, the presence of Hg^{2+} changed the conforma-

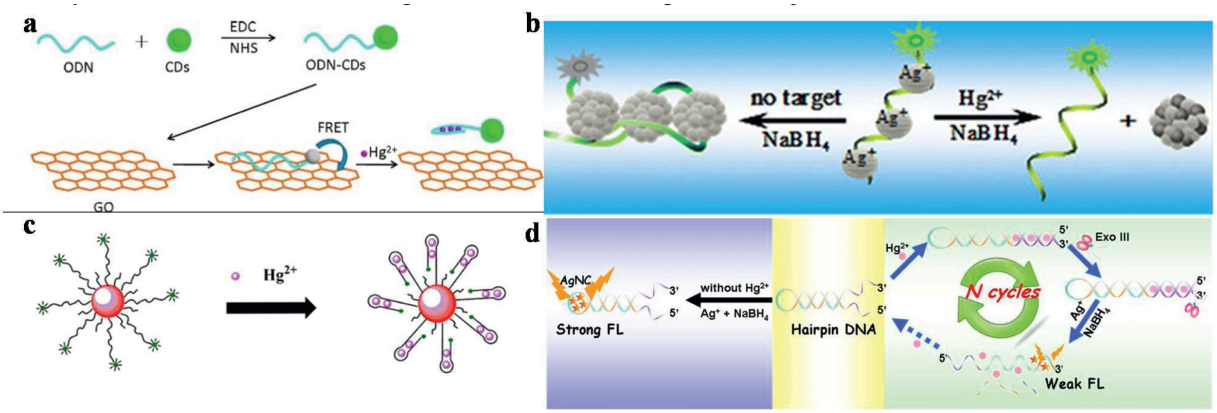

Fig. 8. (a) Schematic illustration of the GO-based sensor system for Hg^{2+} detection. Copied with permission [104]. Copyright 2015, Elsevier. (b) Schematic illustration of fluorescent detection of Hg^{2+} ions by forming Ag/Hg amalgam that suppresses AgNPs growth on a dye-labeled DNA scaffold (FAM-DNA). Copied with permission [110]. Copyright 2013, American Chemical Society. (c) Schematic representation of the sensing mechanism of AuNPs-DNA-FAM for the FL determination of Hg^{2+}. Copied with permission [32]. Copyright 2015, Elsevier. (d) Schematic illustration of Hg^{2+} fluorescent sensing strategy. Copied with permission [111]. Copyright 2015, Elsevier.

tion of DNA sequence, which led to changes of FL signals. In addition, mixing the detection sequence with a short, non-fluorescent sequence at 1:5 can improve the sensitivity to 8 nmol/L of LOD. To further improve the sensitivity, Xu *et al.* introduced exonuclease III (Exo III) cleavage amplification into aiding the FRET-based detection [111]. As designed in Fig. 8d, in the absence of target Hg^{2+} and Exo III, strong FL signals were emitted during the reaction of hairpin DNA-combined $AgNO_3$ with $NaBH_4$. In the presence of Hg^{2+}, the new configuration of Multi-T DNA combined with Hg^{2+} was fabricated, which released Ag^+ to result in the weak FL signals. Simultaneously, Exo III would digest the Hg^{2+}-combined DNA, to release Hg^{2+} for participating the subsequent amplification. As a result, the FL intensity decreased with the increase of Hg^{2+} concentration, exhibiting LOD of 24 pmol/L.

2.5. Other applications

The FRET-based methods can also be employed for detecting other life-related species, monitoring of corresponding process, delivery of drugs, therapy and other applications.

Potentially, DNA nanostructures could provide addressable scaffolds for organizing chromophores (*e.g.*, organic dyes) into networks, which could mimic biological light harvesting complexes. While limitations including flexibilities of DNA scaffolds, variations in dye positions and orientations or poor formation efficiency made synthetic light harvesting inefficient. Nevertheless, the dyes in the crystal experience a more homogeneous environment than reference DNA strands in solution, showing increased quantum yield single-exponential FL decays. This was realized by forming FRET-based DNA crystal systems *via* self-assembling of DNA tensegrity triangles with covalently attached Cy3 and Cy5 [112]. Then, a FRET-based porous silicon (PS) photonic crystal biosensor was constructed for detecting 16S rRNA of actinobacteria. Through DNA hybridization between QDs and AuNPs, the FRET system was formed with QD to act as an emission donor and AuNP as a quencher. With QDs-conjugated probe adhered to the PS layer, FL of PS photonic crystal drastically increased. After adding AuNPs-conjugated complementary 16S rRNA onto QDs-conjugated PS, the FL of QDs decreased, originating from the FRET between QDs and AuNPs through DNA hybridization. As demonstrated, the decreased FL intensity showed a good linear relationship with complementary DNA concentration (Linearity range: 0.25 μmol/L to 10 μmol/L; LOD: 328.7 nmol/L). Unlike traditional FRET systems in liquid system, this platform benefited optical FRET label-free biosensors on Si substrate, which were potential for developing optical biochips [113].

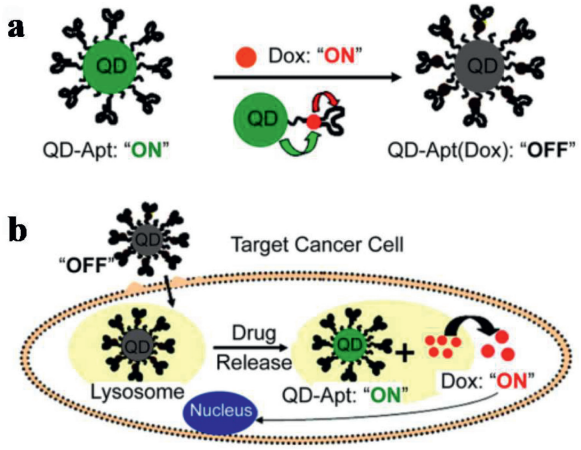

Fig. 9. Schematic representation of Apt-functionalized QDs for combined cancer cell imaging and therapy. (a) Dox is intercalated into DNA Apts on QDs. (b) Apts recognize cell surface markers of a target cancer cell, and Dox is released once the construct is internalized. Reproduced with permission [116]. Copyright 2007, American Chemical Society.

Through changes of FRET-based FL signals, some *in vivo* processes from basic biological to biomedical disciplines could be monitored. This was significant for dynamic studies not only in heterogeneous cellular populations, but also at the single-cell level in real time. For example, single-cell FRET-based biosensors have been developed to monitor cellular energy flux as well [114,115]. Nanomaterial-FRET can also be used for monitoring drug delivery, release, or the corresponding FRET-based processes. For example, QDs coated with Apts against prostate-specific membrane antigen (PSMA) could be used to selectively deliver doxorubicin (Dox) to prostate cancer cells (LNCaP). This can be used for cancer cell detection and treatment. As shown in Fig. 9, the FL emitted from both Dox and QDs was quenched through FRET before cellular entry. This was achieved by intercalating Dox within the A10 Apt, which formed a donor-acceptor of QD-Dox and a donor-quencher of Dox-Apt. Upon cellular entry, biodegradation of PSMA Apt by lysosomal enzymes in the lysosomes can induce releasing of Dox from QD-Apt conjugates. This generated an increased FL from both the Dox and the QD. Therefore, based on the FL signals, the delivery of Dox to the targeted prostate cancer cells was monitored by imaging of

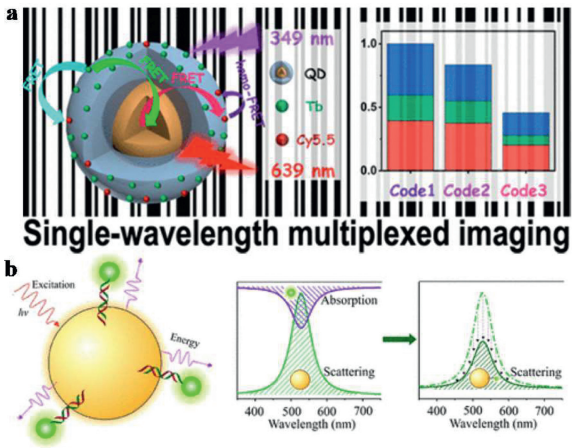

Fig. 10. (a) FRET-modulated multihybrid nanoparticles for brightness-equalized single-wavelength barcoding. Copied with permission [119]. Copyright 2019, American Chemical Society. (b) PRET between AuNP donors and chromophore acceptors. Reproduced with permission [120]. Copyright 2020, American Chemical Society.

cancer cells. This provided an avenue for the design of theranostic nanomaterials to simultaneously detect and treat cancer cells [116]. In addition, with nitrobenzoxadiazolyl derivative (NBD) dyes encapsulated into copolymer micelles, a reversible, light-responsive, dual-color FRET-based system could also be applied to track drug deliveries [117].

Furthermore, the multiple diagnosis based on small molecular biomarkers was also reported. Hai *et al.* prepared a multifunctional AgNPs@GQDs by synergistic *in situ* growth of AgNPs on the complex of tannic acid (TA) and GQDs. This was used for constructing a FRET-based dual-biosensing platform for cancer diagnosis. The nanocomposite exhibited a H_2O_2-responsive degradation, in which Ag^0 was oxidized to Ag^+ along with releasing oxidized TA and GQDs. This degradation induced the suppression of FRET in AgNPs@GQDs, which decreased absorbance and FL intensity for colorimetric/FL dual-mode sensing of H_2O_2. Considering high H_2O_2 level in cancer cells, H_2O_2-responsive degradation of AgNPs@GQDs exhibited good performance for recognition and therapy of cancer cells. The synergistic anticancer effect by Ag^+ and oxidized TA contributed to effective cell death, which could be liberated by GQDs signals [118].

2.6. Mechanism studies of FRET

The mechanism studies of nanoparticle-based FRET system are crucial for improving FRET performance for better applications. This can also provide significant guidance for preparation of nanomaterials to construct new FRET-based systems.

For mechanism studies, Chen *et al.* applied time-resolved and steady-state photoluminescence (PL) spectroscopy and Monte Carlo simulations into holistic photophysical analysis of multidonor-QD-multiacceptor FRET systems. As demonstrated, the FRET efficiency depended on the acceptor number rather than the donor number. This could be used to optimize the PL intensity by adjusting donor numbers and the PL lifetime by changing acceptor numbers, independently. Guided by this rule, different nanoparticle-encoded microbeads were efficiently differentiated within the same view at a single-wavelength excitation (Fig. 10a). This work made a complete understanding of multidonor-acceptor FRET networks on advanced FL sensing and imaging [119].

In addition, Ma *et al.* examined the influence of the distance (d) between the plasmonic nanoparticle and the conjugated molecules on the plasmon resonance energy transfer (PRET) efficiency (η_{PRET}) (Fig. 10b). This was achieved *via* two PRET systems included tetramethylrhodamine (TAMRA) or Cy3 molecules as acceptors and single spherical AuNPs as donors. With excessive TAMRA- or Cy3-labeled dsDNA added, dsDNA was assumed to radially point out from the AuNPs surface to minimize steric hindrance. A donor-acceptor spacer within 12 nm was precisely adjusted by dsDNA sequences. Then, two η_{PRET} systems with varied d-values were obtained *via* reducing scattering intensity of AuNPs. Both experimental and *quasi*-static approximation data demonstrated a d-value-dependent decay function of η_{PRET}, which provided new insights into optimizing PRET-based biochemical sensors [120].

3. FRET processes without nanomaterials involved

Moreover, the nanoparticles are not always required to be involved in FRET process. For example, silica nanomaterials can act as typical excellent matrix for FERT-based detection, which possesses high loading efficiency, low FL background and good biocompatibility. Recently, Shen *et al.* presented a mesoporous silica nanomaterial (MSN)-based chemiluminescence RET (CRET)-nanosensor for the sensitive detection of miRNA (Fig. 11a). The principle of CRET is similar to that of FRET. The CRET efficiency (E) can also be defined in the equation $E = 1/(1 + R^6/{R_0}^6)$, where R_0 is the distance leading to 50% of energy transfer from the donor to the acceptor [121]. In contrast to FRET, CRET occurs by the oxidation of a luminescent substrate without an excitation source. In the experiment, MSNs acted as carriers to load both the donor (horseradish peroxidase, HRP) and the acceptor (a functional DNA duplex). By controlling the energy transfer distance, the donor emission is quenched by the adsorption of the dye on the acceptor DNA. *Via* the competitive hybridization of target miRNA, the FRET system could be destroyed by releasing acceptor DNA from linker DNA. This resulted in emission recovery for quantification of the cancer biomarker of miR-155. With high energy-transfer efficiency, good specificity, favorable biodegradability and low toxicity, this work provided a potential pathway for biological detection and clinical diagnosis [45].

Furthermore, with nanoparticles as FRET matrix, extensive applications on measurements of MMP enzymes and rapid evaluation of anticancer compounds were employed. For example, Qian described a switchable FRET system based on telomerase-responsive MSNs to realize *in situ* “off-on” imaging of intracellular telomerase activity (Fig. 11b) [46]. The fluorescein was entrapped in the mesopores of MSN and covalently immobilized black hole quencher (BHQ) on the inner walls of the mesopores. Then, the detachment of O1 triggered the release of fluorescein to turn “on” its FL. Then, in the presence of telomerase and dNTPs, the designed O1 can be extended and then moves away from the MSN surface. This process was employed *via* the formation of a rigid hairpin-like DNA structure. Thus, the O1 can act as a "biogate" to block and release fluorescein for “off-on” switchable fluorescent imaging. Therefore, a telomerase-responsive biosensor was constructed based on FRET-process on MSN matrix.

For monitoring deubiquitinating enzyme activity, Wang *et al.* present novel Tb-loaded MSNs as a type of nano-probe based on FRET. In this work, Tb-complexes were modified in the pores of the MSNs (MSN-Tb). The emission property of Tb was obviously enhanced *via* the confinement effect of the MSN pores. Then, rhodamine B labeled Ubs (Ub-Rs) were reacted with the aminated MSNs, forming a peptide bond at the exposed carboxyl group on the Ub. Thereby, under the light excitation, FRET occurred from the Tb of the MSN-Tb to the rhodamine B on the Ub-Rs. Then, the peptide bond between MSN-Tb and Ub-Rs was broken after the addition of the UCH-L1 (a model of DUBs). Meanwhile, the FRET effect was cut off, and the emission of the Tb complexes was recovered. Therefore, the prepared MSN probe can be used as a ratio-metric sensor for sensing the DUB (UCH-L1) activity [47].

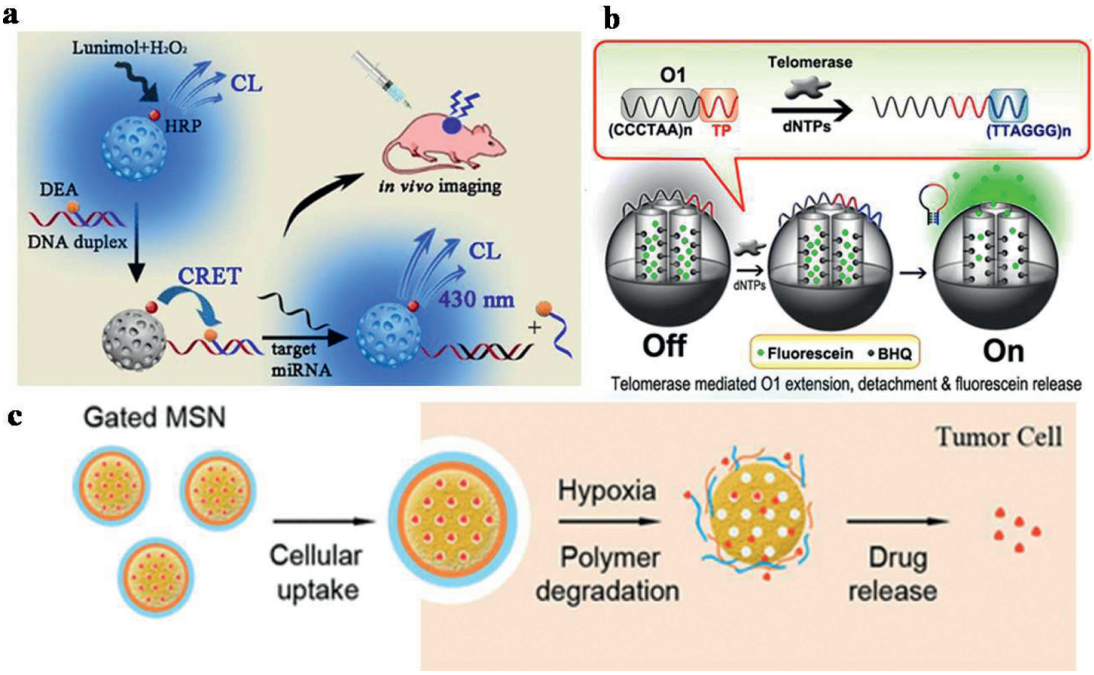

Fig. 11. (a) CRET-based MSNs for the detection of miRNA. Copied with permission [45]. Copyright 2020 American Chemical Society. (b) Switchable fluorescent imaging of intracellular telomerase activity using telomerase-responsive MSNs. Copied with permission [46]. Copyright 2013, American Chemical Society. (c) Gated MSNs for hypoxia-responsive cargo release. Copied with permission [48]. Copyright 2019, American Chemical Society.

Furthermore, MSNs can be used as gatekeepers for hypoxia-responsive cargo release. Lai *et al.* described a versatile FRET-based real-time monitoring system [122]. In this system, MSNs were tethered with coumarin-labeled-cysteine and acted as the drug carrier. A fluorescein isothiocyanate-β-cyclodextrin (FITC-β-CD) acted as redox-responsive molecular valve to block the pores in MSNs. Therefore, a FRET donor-acceptor pair of coumarin and FITC was integrated within the pore-unlocking event. This allowed monitoring of drug releasing from the pores in real-time. The FRET system was established *via* the disulfide bond, which decreased the distance between coumarin and FITC on the surface of MSNs. However, in the presence of glutathione (GSH), the disulfide bond was cleaved and led to the removal of molecular valve. Thus, the release of the drugs was monitored by changes of FRET signal, which entrapped within pores of the MSN nanocarrier. Zhao *et al.* engineered a novel MSN coated by the azobenzene polymer, poly(4,4′-azodianiline) (pDAB) (Fig. 11c). A standard photosensitizer, chlorin e6 (Ce6) was employed as the model cargo to be encapsulated within the MSN. As azobenzene was hydrophobic, an amphiphilic copolymer of Pluronic F68 (F68) was further deposited on its exterior to ensure MSN's good affinity or dispersibility in water. The hypoxia-responsive cargo released from the gated MSN was quantitatively demonstrated in breast cancer cells (MCF-7) using the FRET technique. In this system, coumarin 6 and rhodamine B was selected as the FRET donor and acceptor, respectively [48].

4. Summary and outlook

We have reviewed recently reported nanoparticle-FRET methods for detecting nucleic acids, proteins, heavy metal ions, and other biomarkers both *in vitro* and *in vivo*. Advantages of nanoparticles, including high surface-area-to-volume ratio and unique optical properties, allow them to overcome some limitations on current biological detections. This makes nanotechnology-based assays become an increasingly relevant alternative to traditional techniques for cancer detections. During the biological detections by FRET-based nanoparticles, various nanoparticles were introduced, which could be involved in the FRET process. These kinds of nanoparticles exhibit tunable absorption and high quantum yields. In addition, the nanoparticles could act as the matrix of FRET systems (such as MSNs), which simultaneously deliver chemotherapeutics or photosensitizing agents into cells. The nanoparticle-FRET techniques will be of great importance in FL-based assays for the analysis and real-time monitoring of cellular events in living cells. This would allow more exact and thorough understanding of cellular events. Furthermore, the increased mechanism understanding of the FRET-based techniques would be encouraged. This could be a key biological tool in learning critical lessons about cellular processes, disease progression, and drug therapy. In summary, with the developments on FRET-based techniques, challenges on nanoparticle-FRET detections in body fluid, cells, tissues or living body have been overcome gradually. In the future, researchers in this field are encouraged to further develop nanoparticle-FRET into the rapid diagnosis, prognosis and therapeutics.

Declaration of competing interest

We declare that we have no financial and personal relationships with other people or organizations that can inappropriately influence our work.

Acknowledgments

N. Na gratefully acknowledges the financial support provided by the National Key Research and Development Program of China (No. 2019YFC1805600) and the National Natural Science Foundation of China (NNSFC, No. 21874012) . J. Ouyang is thankful for the financial support provided by the NNSFC (No. 21974010).

References

[1] T. Förster, Ann. Phys. 437 (1948) 55–75.
[2] R. Roy, S. Hohng, T. Ha, Nat. Methods 5 (2008) 507–516.
[3] I.L. Medintz, J.H. Konnert, A.R. Clapp, et al., Proc. Natl. Acad. Sci. U. S. A. 101 (2004) 9612.

[4] I.L. Medintz, A.R. Clapp, H. Mattoussi, et al., Nat. Mater. 2 (2003) 630.
[5] E.R. Goldman, I.L. Medintz, J.L. Whitley, et al., J. Am. Chem. Soc. 127 (2005) 6744.
[6] Y. Wang, Z. Tang, M.A. Correa-Duarte, L.M. Liz-Marzan, N.A. Kotov, J. Am. Chem. Soc. 125 (2003) 2830.
[7] W.R. Algar, N. Hildebrandt, S.S. Vogel, I.L. Medintz, Nat. Methods 16 (2019) 815–829.
[8] F. Patolsky, Y. Weizmann, I. Willner, J. Am. Chem. Soc. 124 (2002) 770.
[9] S. Peng, R. Sun, W. Wang, C. Chen, Chin. Chem. Lett. 29 (2018) 1503–1508.
[10] T. Xiao, W. Zhong, L. Zhou, et al., Chin. Chem. Lett. 30 (2019) 31–36.
[11] J. Zhuang, D. Wang, D. Li, et al., Chin. Chem. Lett. 29 (2018) 1815–1818.
[12] Y. Yan, X. Zhang, X. Zhang, et al., Chin. Chem. Lett. 31 (2020) 1091–1094.
[12] P. Zhou, P. Lv, L. Yu, et al., Chin. Chem. Lett. 30 (2019) 1067–1070.
[14] M. Li, J. Chen, J. Pan, et al., Chin. Chem. Lett. 30 (2019) 541–544.
[15] M. Elangovan, R.N. Day, A. Periasamy, J. Microsc. 205 (2002) 3–14.
[16] A. Miyawaki, Y. Niino, Mol. Cell 58 (2015) 632–643.
[17] B.T. Bajar, E.S. Wang, A.J. Lam, et al., Sci. Rep. 6 (2016) 20889.
[18] B. Hochreiter, A.P. Garcia, J.A. Schmid, Sensors 15 (2015) 26281–26314.
[19] S.J. Sahl, S.W. Hell, S. Jakobs, Nat. Rev. Mol. Cell Bio. 18 (2017) 685–701.
[20] R. Moussa, A. Baierl, V. Steffen, et al., J. Biotechnol. 191 (2014) 250–259.
[21] L. Schärfen, M. Schlierf, Methods 169 (2019) 11–20.
[22] E.A. Booth, J. Thorner, Methods Cell Biol 136 (2016) 35–56.
[23] R.G. Sturmey, P.J. O'Toole, H.J. Leese, Reproduction 132 (2006) 829–837.
[24] D.R. Davydov, N.Y. Davydova, J.R. Halpert, Biochemistry 47 (2008) 11348–11359.
[25] H. Fernando, J.R. Halpert, D.R. Davydov, Biochemistry 45 (2006) 4199–4209.
[26] Y.E. Choi, J.W. Kwak, J.W. Park, Sensors 10 (2010) 428–455.
[27] J. Yao, M. Yang, Y. Duan, Chem. Rev. 114 (2014) 6130–6178.
[28] M.H.W. Stopel, J.C. Prangsma, C. Blum, V. Subramaniam, RSC Adv. 3 (2013) 17440–17445.
[29] S.R. Sturzenbaum, M. Hockner, A. Panneerselvam, et al., Nat. Nanotechnol. 8 (2013) 57–60.
[30] C.Y. Zhang, H.C. Yeh, M.T. Kuroki, T.H. Wang, Nat. Mater. 4 (2005) 826–831.
[31] I.L. Medintz, A.R. Clapp, H. Mattoussi, et al., Nat. Mater. 2 (2003) 630–638.
[32] G.K. Wang, Y.F. Lu, C.L. Yan, Y. Lu, Sens. Actuators B: Chem. 211 (2015) 1–6.
[33] C.C. You, O.R. Miranda, B. Gider, et al., Nat. Nanotechnol. 2 (2007) 318–323.
[34] C. Bremer, C.H. Tung, R. Weissleder, Nat. Med. 7 (2001) 743–748.
[35] B.E. Turk, L.L. Huang, E.T. Piro, L.C. Cantley, Nat. Biotechnol. 19 (2001) 661–667.
[36] K.S. Novoselov, A.K. Geim, S.V. Morozov, et al., Science 306 (2004) 666–669.
[37] A.K. Geim, K.S. Novoselov, Nat. Mater. 6 (2007) 183–191.
[38] M.C. Liu, C.L. Chen, J. Hu, X.L. Wu, X. Wang, J. Phys. Chem. C 115 (2011) 25234–25240.
[39] M. Li, Q. Liu, Z.J. Jia, et al., Carbon 67 (2014) 185–197.
[40] C.L. Weaver, J.M. LaRosa, X.L. Luo, X.T. Cui, ACS Nano 8 (2014) 1834–1843.
[41] J. Hu, M.H. Liu, C.Y. Zhang, ACS Nano 13 (2019) 7191–7201.
[42] L. He, D.Q. Lu, H. Liang, et al., ACS Nano 11 (2017) 4060–4066.
[43] J. Gao, H. Zhang, Z. Wang, Analyst 145 (2020) 3535–3542.
[44] G. Su, M. Zhu, M. Xu, et al., Chem. Commun. 56 (2020) 13583–13586.
[45] X.T. Shen, W. Xu, J.B. Guo, J. Ouyang, N. Na, ACS Sens. 5 (2020) 2800–2805.
[46] R. Qian, L. Ding, H. Ju, J. Am. Chem. Soc. 135 (2013) 13282–13285.
[47] Y.Y. Liang, J. Zhang, H. Cui, et al., Chem. Commun. 56 (2020) 3183–3186.
[48] Q. Yan, X. Guo, X. Huang, et al., ACS Appl. Mater. Interfaces 11 (2019) 24377–24385.
[49] Y. Li, D.L. Jia, W. Ren, F. Shi, C.H. Liu, Adv. Funct. Mater. 29 (2019) 1903191.
[50] W. Song, H.J. Zhang, Y.H. Liu, C.L. Ren, H.L. Chen, Chin. Chem. Lett. 28 (2017) 1675–1680.
[51] W. Yu, M. Shevtsov, X. Chen, H. Gao, Chin. Chem. Lett. 31 (2020) 1366–1374.
[52] C.H. Liu, L.J. Chang, H.H. Wang, Anal. Chem. 86 (2014) 6095–6102.
[53] W.M. Howell, Methods Mol. Biol. 335 (2006) 33–41.
[54] C.Y. Zhang, H.C. Yeh, M.T. Kuroki, T.H. Wang, Nat. Mater. 4 (2005) 826–831.
[55] H.H. Chen, K.W. Leong, Nanomedicine 1 (2006) 119–122.
[56] C.Y. Zhang, L.W. Johnson, Anal. Chem. 78 (2006) 5532–5537.
[57] D.J. Zhou, L.M. Ying, X. Hong, et al., Langmuir 24 (2008) 1659–1664.
[58] W.R. Algar, U.J. Krull, Anal. Chim. Acta 581 (2007) 193–201.
[59] H. Peng, L.J. Zhang, T.H.M. Kjallman, C. Soeller, J. Travas-Sejdic, J. Am. Chem. Soc. 129 (2007) 3048–3049.
[60] J. Lee, Y. Choi, J. Kim, E. Park, R. Song, ChemPhysChem 10 (2009) 806–811.
[61] J.C. Park, S.Y. Choi, M.Y. Yang, et al., ACS Appl. Mater. Interfaces 11 (2019) 33525–33534.
[62] J. Guo, X. Qiu, C. Mingoes, et al., ACS Nano 13 (2019) 505–514.
[63] K. Bartnik, A. Barth, M. Pilo-Pais, et al., J. Am. Chem. Soc. 142 (2020) 815–825.
[64] D.S. Seferos, D.A. Giljohann, H.D. Hill, A.E. Prigodich, C.A. Mirkin, J. Am. Chem. Soc. 129 (2007) 15477–15479.
[65] C.H.J. Choi, L.L. Hao, S.P. Narayan, E. Auyeung, C.A. Mirkin, Proc. Natl. Acad. Sci. U. S. A. 110 (2013) 7625–7630.
[66] J.I. Cutler, E. Auyeung, C.A. Mirkin, J. Am. Chem. Soc. 134 (2012) 1376–1391.
[67] D.A. Giljohann, D.S. Seferos, P.C. Patel, et al., Nano Lett 7 (2007) 3818–3821.
[68] N.L. Rosi, D.A. Giljohann, C.S. Thaxton, Science 312 (2006) 1027–1030.
[69] P.C. Patel, D.A. Giljohann, W.L. Daniel, et al., Bioconjugate Chem. 21 (2010) 2250–2256.
[70] J.M. Levsky, R.H. Singer, J. Cell Sci. 116 (2003) 2833–2838.
[71] M.D. Massich, D.A. Giljohann, A.L. Schmucker, P.C. Patel, C.A. Mirkin, ACS Nano 4 (2010) 5641–5646.
[72] M.D. Massich, D.A. Giljohann, D.S. Seferos, et al., Mol. Pharmaceutics 6 (2009) 1934–1940.
[73] D. Zheng, D.S. Seferos, D.A. Giljohann, P.C. Patel, C.A. Mirkin, Nano Lett 9 (2009) 3258–3261.
[74] X. Zhang, N. Ying, C. Shen, G. Cui, J. Nanosci. Nanotechnol. 17 (2017) 1053–1060.
[75] C. Zhu, J. Yang, J. Zheng, et al., Anal. Chem. 91 (2019) 15599–15607.
[76] B.B. Haab, Curr. Opin. Biotechnol. 17 (2006) 415–421.
[77] X. Wang, Y. Xia, Y. Liu, et al., Chem. Eur. J. 18 (2012) 7189–7195.
[78] W.R. Algar, D. Wegner, A.L. Huston, J. Am. Chem. Soc. 134 (2012) 1876–1891.
[79] Q. Wei, M. Lee, X. Yu, et al., Anal. Biochem. 358 (2006) 31–37.
[80] Y. Choi, M. Pinto, Appl. Immunohistochem. Mol. Morphol. 13 (2005) 19–24.
[81] Y. Omoto, H. Iwase, Cancer Sci 106 (2015) 337.
[82] K.D. Wegner, Z. Jin, S. Linden, T.L. Jennings, N. Hildebrandt, ACS Nano 7 (2013) 7411–7419.
[83] J. Kim, S. Kwon, J.K. Park, I. Park, Biosens. Bioelectron. 55 (2014) 209–215.
[84] D. Shitrit, B. Zingerman, A.B. Shitrit, D. Shlomi, M.R. Kramer, Oncologist 10 (2005) 501–507.
[85] M.J. Duffy, S. Shering, F. Sherry, E. McDermott, N.O. Higgins, Int. J. Biol. Markers 15 (2000) 330–333.
[86] A. Keshaviah, S. Dellapasqua, N. Rotmensz, et al., Ann. Oncol. 18 (2007) 701–708.
[87] S. Nath, P. Mukherjee, Trends Mol. Med. 20 (2014) 332–342.
[88] S. Ge, L. Ge, M. Yan, et al., Biosens. Bioelectron. 43 (2013) 425–431.
[89] G. Yang, Q. Zhang, L. Ma, et al., Anal. Chim. Acta. 1098 (2020) 133–139.
[90] Y. Zhan, S. Ling, H. Huang, et al., Angew. Chem. Int. Ed. 60 (2021) 2637–2642.
[91] S.M. Yoo, S.Y. Lee, Trends Biotechnol 34 (2016) 7–25.
[92] X.H. Tan, Y.B. Li, Y. Liao, H.Z. Liu, Sci. Rep. 10 (2020) 20710.
[93] I.L. Medintz, A.R. Clapp, F.M. Brunel, et al., Nat. Mater. 5 (2006) 581–589.
[94] R. Gill, L. Bahshi, R. Freeman, I. Willner, Angew. Chem. Int. Ed. 47 (2008) 1676–1679.
[95] H. Yuan, H. Zhao, K. Peng, et al., ACS Appl. Mater. Interfaces 12 (2020) 21263–21269.
[96] Y. Shen, T. Wu, Y. Zhang, et al., Anal. Chem. 92 (2020) 13396–13404.
[97] N. Xia, F. Feng, C. Liu, et al., Talanta 192 (2019) 500–507.
[98] C. Garza-Lombo, Y. Posadas, L. Quintanar, M.E. Gonsebatt, R. Franco, Antioxid. Redox Signal. 28 (2018) 1669–1703.
[99] Y.Y. Qi, F.R. Xiu, G. Yu, L.L. Huang, B.X. Li, Biosens. Bioelectron. 87 (2017) 439–446.
[100] R.Y. Wang, X.H. Zhou, H.C. Shi, Y. Luo, Biosens. Bioelectron. 78 (2016) 418–422.
[101] X. Li, J.Q. Xie, B.Y. Jiang, R. Yuan, Y. Xiang, ACS Appl. Mater. Interfaces 9 (2017) 5733–5738.
[102] J. Lehel, D. Zwillinger, A. Bartha, K. Lányi, P. Laczay, Environ. Sci. Pollut. Res. Int. 24 (2017) 25372–25382.
[103] R. Akhbarizadeh, F. Moore, B. Keshavarzi, Environ. Pollut. 232 (2018) 154–163.
[104] X. Cui, L. Zhu, J. Wu, et al., Biosens. Bioelectron. 63 (2015) 506–512.
[105] M. Wu, R. Kempaiah, P.J.J. Huang, V. Maheshwari, J. Liu, Langmuir 27 (2011) 2731–2738.
[106] H.N. Abdelhamid, H.F. Wu, Microchim. Acta 182 (2015) 1609–1617.
[107] C. Lu, P.J.J. Huang, Y.B. Ying, J.W. Liu, Biosens. Bioelectron. 79 (2016) 244–250.
[108] J.S. Li, H. Wang, Z.K. Guo, et al., Talanta 162 (2017) 46–51.
[109] X.W. Zuo, H.G. Zhang, Q. Zhu, W.F. Wang, X.G. Chen, Biosens. Bioelectron. 85 (2016) 464–470.
[110] L. Deng, X.Y. Ouyang, J.Y. Jin, et al., Anal. Chem. 85 (2013) 8594–8600.
[111] M.D. Xu, Z.Q. Gao, Q.H. Wei, G.N. Chen, D.P. Tang, Biosens. Bioelectron. 79 (2016) 411–415.
[112] J.S. Melinger, R. Sha, C. Mao, N.C. Seeman, M.G. Ancona, J. Phys. Chem. B 120 (2016) 12287–12292.
[113] H. Zhang, J. Lv, Z. Jia, Sensors 17 (2017) 1078.
[114] M. Willemsel, E. Janssen, F. de Lange, B. Wieringa, J. Fransen, Nat. Biotechnol. 25 (2007) 170–172.
[115] S. Zadran, S. Standley, K. Wong, et al., Appl. Microbiol. Biotechnol. 96 (2012) 895–902.
[116] V. Bagalkot, L. Zhang, E. Levy-Nissenbaum, et al., Nano Lett. 7 (2007) 3065–3070.
[117] L.X. Yu, Y. Liu, S.C. Chen, Y. Guan, Y.Z. Wang, Chin. Chem. Lett. 25 (2014) 389–396.
[118] X. Hai, Y.W. Li, K.X. Yu, et al., Chin. Chem. Lett. 32 (2021) 1215–1219.
[119] C. Chen, B. Corry, L. Huang, N. Hildebrandt, J. Am. Chem. Soc. 141 (2019) 11123–11141.
[120] J. Ma, M.X. Gao, H. Zuo, et al., Anal. Chem. 92 (2020) 14278–14283.
[121] L. Stryer, R.P. Hangland, Proc. Natl. Acad. Sci. U. S. A. 58 (1967) 719.
[122] J.P. Lai, B.P. Shah, E. Garfunkel, K.B. Lee, ACS Nano 7 (2013) 2741–2750.